

## AN INVESTIGATION ON THE SUITABLE CONSTITUTIVE LAW FOR MODELLING JAKARTA RED CLAY

GOUW Tjie-Liong <sup>1</sup>

**ABSTRACT:** Having the origin from the sedimentation of volcanic materials, many experienced Indonesian geotechnical engineers have long suspected that Jakarta reddish and grayish clay may have different characteristics compared to other clayey soils known in many geotechnical text books. Despite of carefully derived design parameters, experiences in the execution of deep excavation, be it open cut slope or protected excavation by either contiguous bored pile or diaphragm walls, often show that the performance of the geotechnical structures were better than predicted by the available design geotechnical software. Although, some engineers have started using more advanced constitutive soil models, such as: Hyperbolic and Cam Clay models. Undoubtedly, many engineers still use the bilinear Mohr-Coulomb model in their analysis. So far, to the author knowledge, there is no published paper discussing about the suitability of the soil models for modelling Jakarta red clay, in particular. Therefore, the author tried to find out which soil constitutive models can better predict the behavior of the Jakarta reddish/grayish clay. Available models in PLAXIS software, e.g.; Mohr-Coulomb, Hardening (hyperbolic), and Soft Soil models, were tried by simulating isotropically consolidated undrained triaxial test and compared it with the actual test data. At this stage it was found that none of the model can correctly predict the stress strain curve neither the correct stress path.

**Keywords:** Volcanic Origin Clay, Jakarta Clay, Mohr Coulomb Model, Hardening Soil Model, Soft Soil Model, Plaxis

### INTRODUCTION

Geologically, Jakarta reddish and greyish, very often cemented, clay was formed from the sedimentation of volcanic materials. Despite of using carefully derived soil parameters, experiences in the execution of deep excavation, be it open cut slope or protected excavation by either contiguous bored pile or diaphragm walls, often show that the performance of the geotechnical structures were better than predicted by the available design geotechnical software. It was suspected that the discrepancies may due to the fact that many engineers still use the elastic-perfectly plastic Mohr-Coulomb model in their analysis. However, when more advance soil model, either Cam Clay or Hyperbolic model, is applied, the prediction is still inferior compared to the actual performance. The author finds that it is really a challenge to find out which constitutive model suit the behavior of Jakarta reddish and greyish clay. With that in mind the author tried the Mohr-Coulomb, Hardening (hyperbolic) and soft soil models available in Plaxis software to simulate isotropically consolidated undrained triaxial test and compared it with the actual test data

### ACTUAL TEST DATA

A set of CIU (isotropically consolidated undrained) triaxial tests were conducted on undisturbed reddish clay samples obtained from a depth of 2.0 to 2.5m. Figures 1 to 4 show the test results. Oedometer test was also performed and the result is presented in Fig. 5.

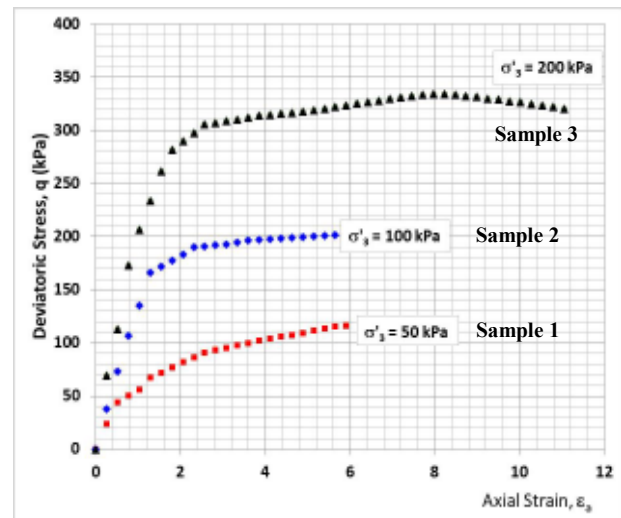


Fig. 1 The Stress Strain Curve

<sup>1</sup> Senior Lecturer and Geotechnical Consultant, Binus University, Jakarta, Indonesia, email: gouw3183@binus.ac.id

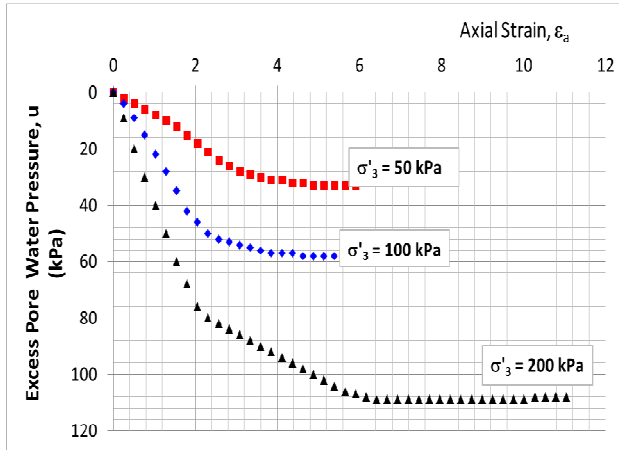


Fig. 2 Excess Pore water Pressures

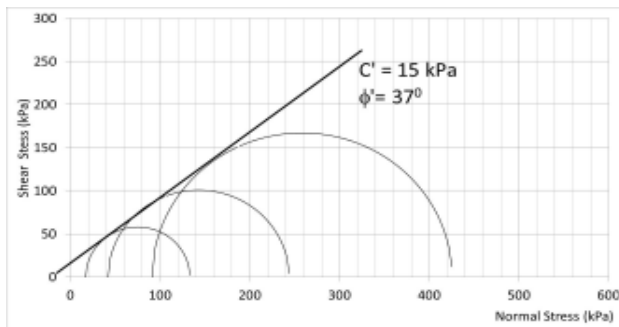


Fig. 3 Mohr Coulomb Effective Shear Strength

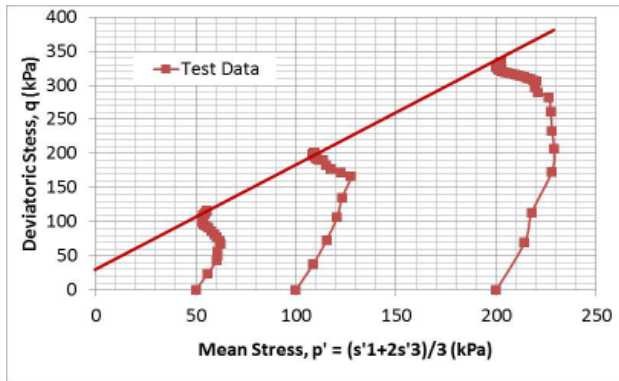


Fig. 4 Test Data Effective Stress Path

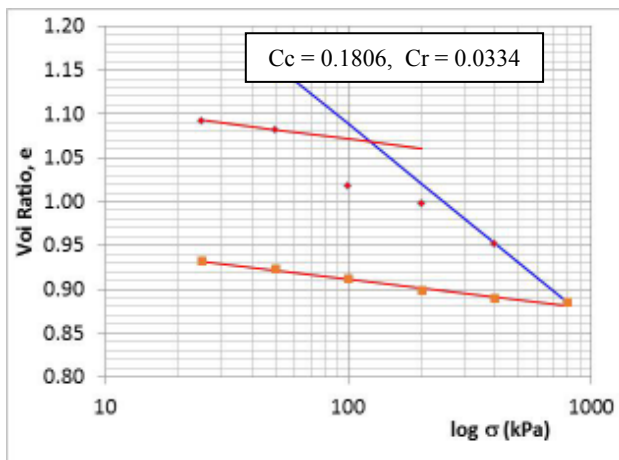


Fig. 5 Oedometer Test Result

## DERIVATION OF MODEL PARAMETERS

### Mohr Coulomb Model Parameters

Figure 6 shows the derivation of  $E_{50}$ , i.e. soil stiffness or secant modulus obtained from 50% of maximum deviatoric stress, divided by the corresponding shear strain.

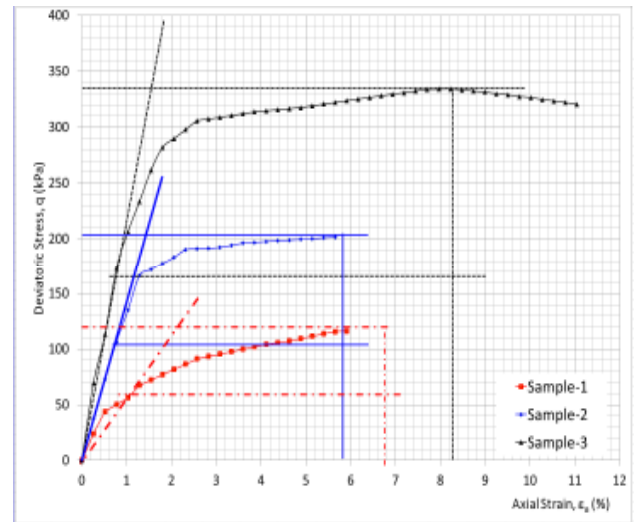


Fig. 6 Derivation of Soil Stiffness,  $E_{50}$

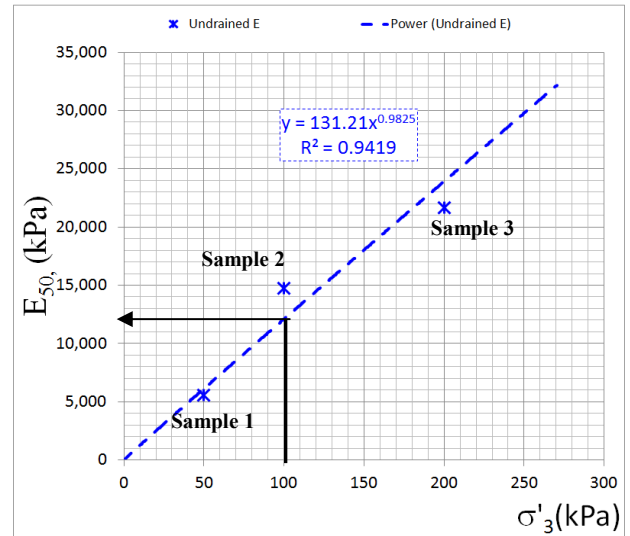


Fig. 7 Determination of  $E_{50}^{ref}$  ( $E_{50}$  at  $P_{ref} = 100$  kPa)

The  $E_{50}$  stiffness obtained from each sample is then plotted against the corresponding confining pressure. Then the  $E_{50}$  at reference confining pressure of 100 kPa is determined (Fig. 7),  $E_{50}^{ref} = 12,105$  kPa, and the effective stiffness value is calculated from the following formula:

$$E'_{50} = \frac{2(1+v')}{3} E_{50} \quad (1)$$

where  $v' =$  drained Poisson' ratio  $\approx 0.30-0.35$ , taking  $v' = 0.3$ , then:

$$E'_{50}{}^{ref} = \frac{2}{3} (1+0.3) \times 12,105 \approx 10,500 \text{ kPa}$$

The derived Mohr Coulomb model parameters to be applied in Plaxis are:

- $c' = 15 \text{ kPa}$ ,  $\phi' = 37^\circ$
- dilation angle,  $\psi = 0^\circ$
- $E'_{50}{}^{\text{ref}} = 10500 \text{ kPa}$
- drained Poisson ratio is taken as 0.3

### Hardening Soil Model Parameters

The hardening soil model used in Plaxis originated from hyperbolic model developed by Duncan and Chang (1970, 1980). In order to utilize the method, first the stress strain curves must be idealized into hyperbolic equation. The process is explained in Fig. 8.

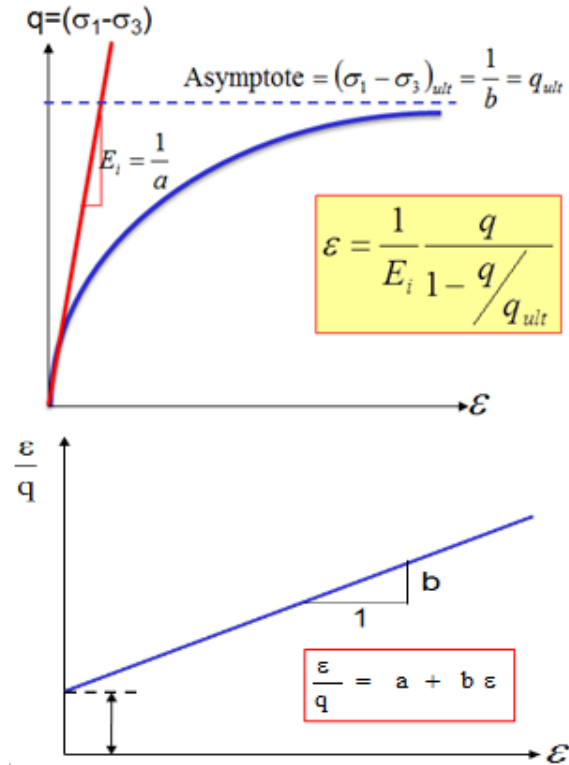


Fig. 8 Process to develop Hyperbolic Equation

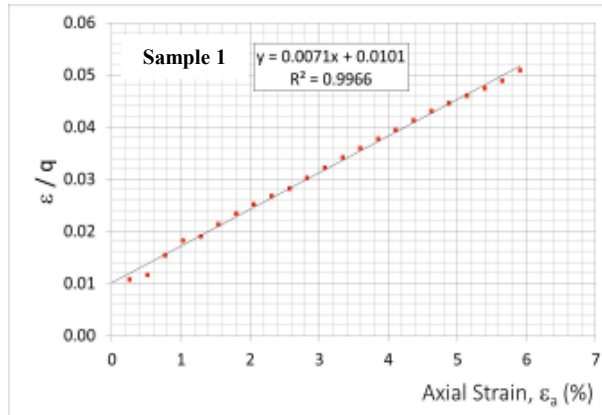


Fig. 9 Derivation of Hyperbolic Parameters of Sample 1

Figure 9 shows sample 1 plot of strain/deviatoric stress against axial strain obtained from stress strain curve presented in Fig. 1. By regression analysis the linearization of a hyperbolic equation for sample 1 is obtained, i.e.,

$$\frac{\epsilon}{q} = a + b\epsilon \quad (2)$$

$$\frac{\epsilon}{q} = 0.0101 + 0.0071\epsilon \quad (2a)$$

Equation (2) can be modified into:

$$q = \frac{\epsilon}{a + b\epsilon} \quad (3)$$

For sample 1, it then becomes:

$$q = \frac{\epsilon}{0.0101 + 0.0071\epsilon} \quad (3a)$$

From equation (3), a hyperbolic curve showing the relation of stress strain ( $q, \epsilon$ ) curve can then be constructed, to approximate the test data. In a similar way, the hyperbolic curve emulating the test data for sample 2 and 3 can also be constructed. Figure 10 shows the results of the derived hyperbolic curves for all three samples tested.

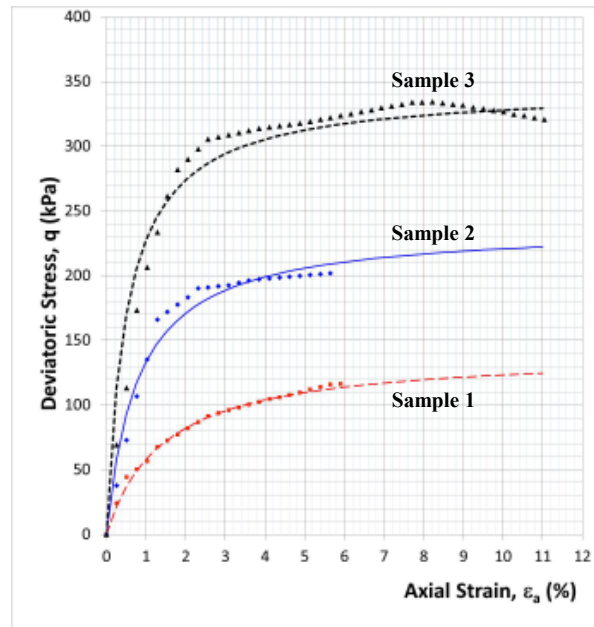


Fig. 10 Hyperbolic Approximation of Test Data

As presented in Fig. 8, once the hyperbolic linearization equation is obtained, the ultimate shear stress and the initial stiffness (Young's modulus) can then be calculated. For sample 1,

Equation (1a) gives:  $a = 0.0101$  and  $b = 0.0071$

$$q_{ult} = \frac{1}{b} \quad (4)$$

$$q_{ult} = 1/b = 1/0.0071 = 140.8 \text{ kPa}$$

$$E_i = \frac{1}{a} \quad (5)$$

Note that the  $E_i$  value obtained from equation (5) needs to be multiplied by 100 if the strain is plotted and evaluated in percentage. For this sample 1,

$$E_i = 1/a \times 100 = 1/0.0101 \times 100 = 9901 \text{ kPa}$$

A failure ratio,  $R_f$ , defined as the ratio of maximum deviatoric stress achieved during the triaxial test,  $q_f$ , and the derived ultimate stress,  $q_{ult}$ , is then need to be calculated,

$$R_f = \frac{q_f}{q_{ult}} \quad (6)$$

the max shear stress achieved for sample 1 is 116 kPa, hence:

$$R_f = q_f/q_{ult} = 116/140.8 = 0.82$$

From all the above, the undrained secant modulus,  $E_{50}$ , can then be calculated by using the following formula:

$$E_{50} = \frac{E_i(2 - R_f)}{2} \quad (7)$$

for sample 1,  $E_{50} = 9901(2 - 0.82)/2 = 5822 \text{ kPa}$

The drained secant modulus,  $E'_{50}$ , is then derived:

$$E'_{50} = \frac{2(1 + \nu')}{3} E_{50} \quad (1)$$

with  $\nu' =$  drained Poisson's ratio  $\approx 0.30 - 0.35$

for sample 1,  $E'_{50} = 2/3(1+0.3) \times 5822 = 5046 \text{ kPa}$

With the same procedures, the values for sample 2 and sample 3 is obtained and all parameters are tabulated in Table 1 below,

Table 1 – Derived Parameters from Hyperbolic Model

		Undrained			Drained		
$\sigma'_{30}$	$q_{ult}$	$q_f$	$R_f$	$E_i$	$E_{50}$	$\nu'$	$E'_{50}$
kPa	kPa	kPa	-	kPa	kPa	-	kPa
50	140.8	116.0	0.82	9,901	5,822	0.3	5,046
100	238.1	201.7	0.85	30,303	17,468	0.3	15,139
200	344.8	334.4	0.97	66,667	34,345	0.3	29,766

The result above shows that both undrained and drained stiffness values are increasing with the effective confining pressures, notated as  $\sigma'_{30}$  here. Plaxis used a reference confining pressure,  $P_{ref}$ , of 100 kPa as the reference value, and the resulting stiffness value is notated as  $E_{50}^{ref}$ . To find this  $E_{50}^{ref}$  value, all the  $E$  values are plotted against the corresponding confining pressures and the  $E_{50}^{ref}$  is derived as shown in Fig. 11.

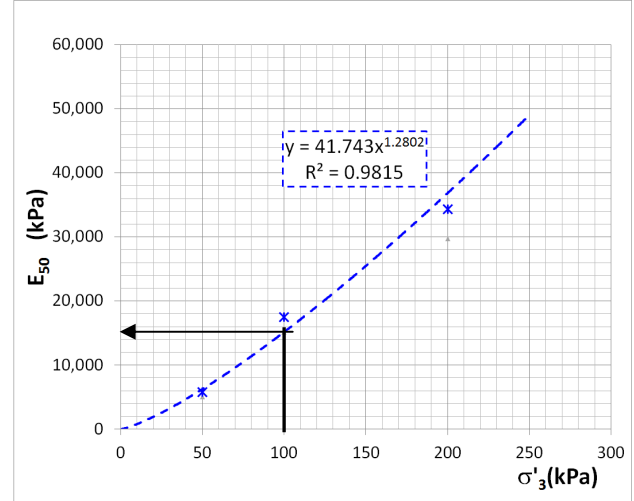


Fig. 10 Derivation of  $E_{50}^{ref}$

Reading from Fig. 10 at confining pressure of 100 kPa, the reference stiffness, can be determined:

$$E_{50}^{ref} = 15,170 \text{ kPa}$$

And using equation (7),

$$E'_{50}^{ref} = 2/3(1+0.3) \times 15170 \approx 13,150 \text{ kPa}$$

Other than  $R_f$  and  $E_{50}^{ref}$  values, the hardening soil model also need the input the oedometer stiffness,  $E_{oed}$ , and the stiffness modulus of unloading reloading,  $E_{ur}$ . These values, can be derived with from oedometer test.

The oedometer test results on the same undisturbed samples, is presented in Figure 5. Instead of the conventional  $e$ - $\log \sigma$  plot, the oedometer curves is re-plotted in the form of axial strain,  $\epsilon$ , vs applied pressure, in a linear scale as presented in Fig. 11.

The oedometer modulus is then obtained from the slope of the loading curve in Fig. 11.

$$E_{oed} = \Delta \sigma / \Delta \epsilon = (800-200) / (0.111-0.063) = 12,500 \text{ kPa}$$

The unloading oedometer modulus is obtained from the unloading part.

$$E_{oed\_unload} = \Delta \sigma / \Delta \epsilon = (800-100)/(0.111-0.1) = 63,640 \text{ kPa}$$

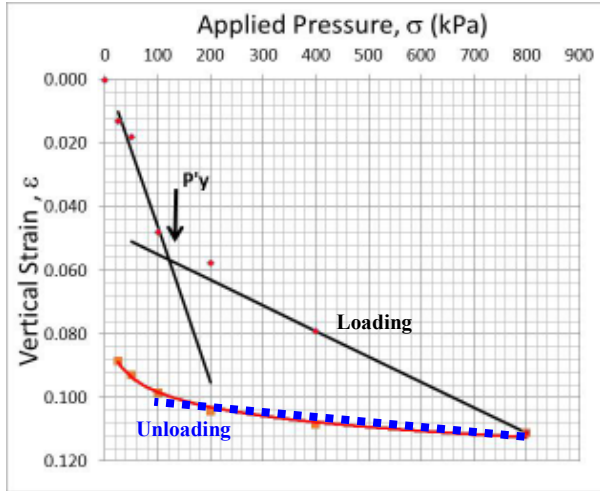


Fig. 11 Oedometer Test for Derivation of  $E_{oed}$

The ratio of the load unload oedometer modulus is:

$$R = E_{oed\_unload} / E_{oed} \quad (8)$$

$$R = 63,460 / 12,500 \approx 5$$

This is also roughly equal to the ratio of compression index,  $C_c$ , over the re-compression index,  $C_r$ , derived from the conventional  $e$ - $\log \sigma$  plot (see Fig. 5)

$$R = C_c / C_r = 0.1806 / 0.0334 = 5.4$$

Taking  $R = 5.25$ , the unloading reloading modulus,  $E_{ur}$ , can be determined as:

$$E_{ur} = R \times E'_{50}{}^{ref} = 5.25 \times 13150 \approx 69,000 \text{ kPa}$$

The hyperbolic model or hardening soil model in Plaxis uses Mohr Coulomb shear strength parameters. So, the summary of the parameters for the hardening soil model is as follows:

- $c' = 15 \text{ kPa}$ ,  $\phi' = 37^\circ$
- dilation angle,  $\psi = 0^\circ$
- drained Poisson ratio,  $\nu' = 0.3$
- $E'_{50}{}^{ref} \approx 13,000 \text{ kPa}$
- $E_{oed} = 12,500 \text{ kPa}$
- $E_{ur} = 69,000 \text{ kPa}$

#### Soft Soil Model Parameters

Soft soil model is one of the models available in Plaxis recommended for analyzing compression load, especially for soft soils. The parameters are generally derived from oedometer test, or from triaxial consolidation test.

In this soft soil model, the oedometer test is not plotted in a conventional  $e$ - $\log \sigma$  plot, but it is plotted in the form of axial strain,  $\epsilon$ , vs natural logarithm of pressure,  $\ln \sigma$ . The curve is presented in Fig. 12 below,

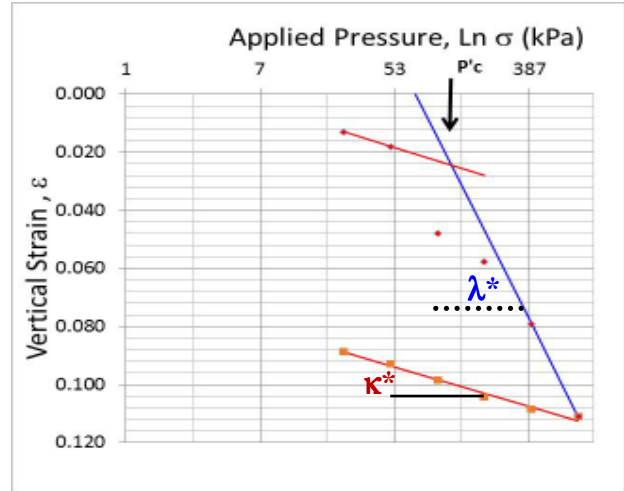


Fig. 12 Oedometer Test for Derivation of  $\lambda^*$  and  $\kappa^*$ .

The slope of the virgin compression line, is notated as  $\lambda^*$  and the slope of the unloading path is termed as  $\kappa^*$ . These two parameters serve as the input on the stiffness of the soil. From the same sample in this case study, those stiffness parameters are:

$$\lambda^* = 0.0462 \text{ and } \kappa^* = 0.0068$$

The strength parameter input for soft soil model is the Mohr-Coulomb strength parameters.

## SIMULATION WITH PLAXIS SOFTWARE

Simulations of the triaxial test were then run in PLAXIS 2D software by employing Mohr Coulomb, Hardening Soil and Soft Soil Model. The triaxial sample is modelled in its real size by employing a 15 nodal axisymmetric model as shown in Fig. 13. The results are then compared with the actual data used in this case study.

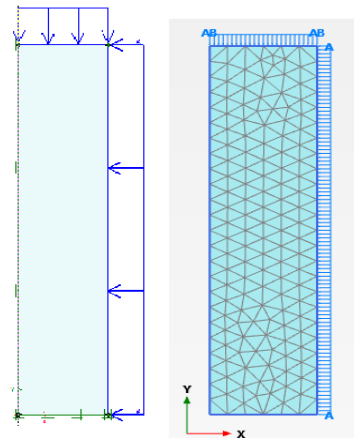


Fig. 13 Axisymmetric Model Triaxial Test

Figure 14 to 16 shows the outcomes of the simulation. Figure 14 shows the stress strain curve, Figure 15 shows the pore water pressure, and Figure 16 shows the stress path.

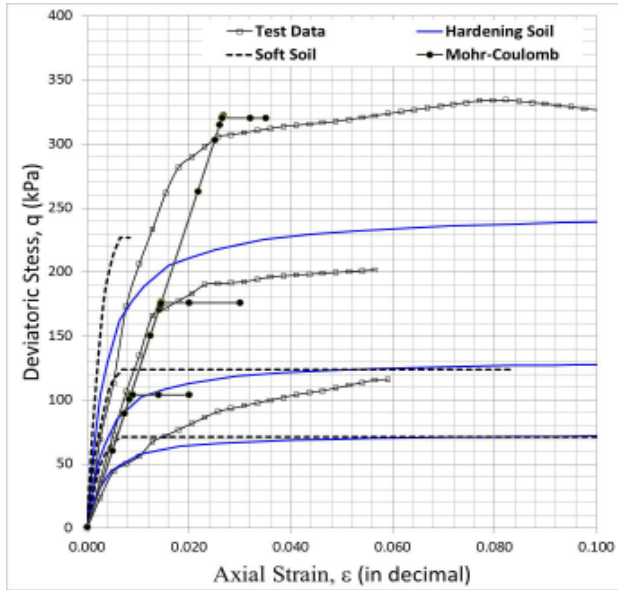


Fig. 14 Stress Strain Curve of Various Soil Models vs. Actual Data

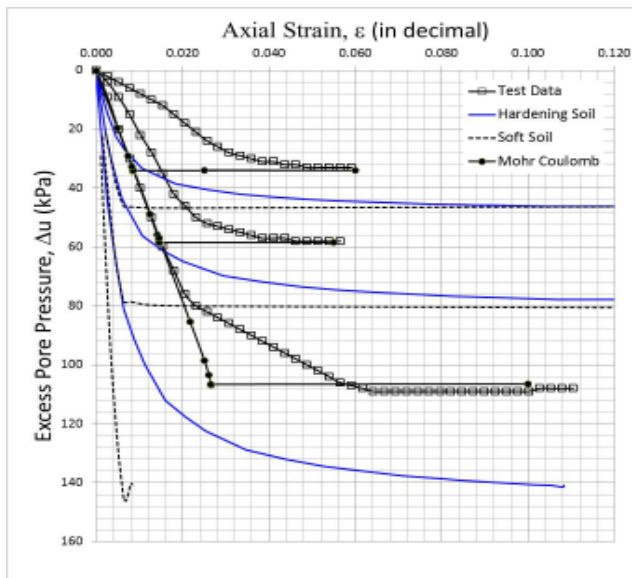


Fig. 15 Excess Pore Water Pressures of Various Soil Models vs. Actual Data

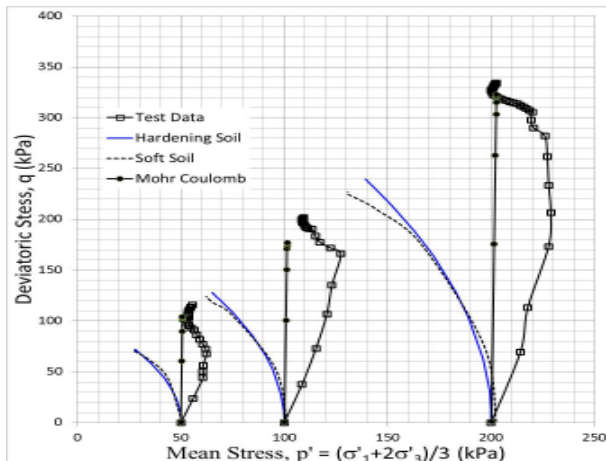


Fig. 16 Stress Paths of Various Soil Models vs. Actual Data

## DISCUSSIONS

The results of the finite element simulation by three soil models, i.e. Mohr Coulomb, Hardening Soil, and Soft Soil models, show that:

Figure 14 show that the hardening soil model gives a more realistic shape of the stress strain curve. The soft soil model appears to give a stiffer stress strain response compared to the hardening soil model. The stress strain curves of Mohr Coulomb (MC) model appear to be linear from the start of the loading until plastic failure occurred; this is in line with the assumption of the MC model. Despite of different confining pressures, MC model always give the same straight line response until it reaches failure level. Both hardening soil and soft soil models under predict the ultimate strength. MC model can approximate the failure load better, but the strain prediction is far from reality. None of the three models can predict the stress strain curve of the actual data correctly.

Figure 15 shows that hardening soil and soft soil models over predict the magnitude of the excess pore pressure. MC can predict the ultimate magnitude of the excess pore water pressure better, but for a strain level below the ultimate strain, the excess pore water pressure is also over predicted. As in the stress strain curve, despite of different confining pressures, MC model always give the same straight line response until it reaches ultimate excess pore water pressures. The shape of the pore water pressure response is better approached by hardening soil, but, as previously said, it still over predicts the magnitude. The response of the soft soil model is the worse in this case.

Figure 16 shows that the stress path of the MC model is always vertically upward, which is not correct. The hardening soil and the soft soil model give the stress path similar to normally consolidated clay. However, none of the models can mimic the stress path of the actual Jakarta reddish clay.

The author also tried to simulate the triaxial test by giving a pre-consolidation pressure (indicated as POP in Plaxis) and also tried to give over-consolidation ratio of varying degrees. It still appears that none of the models can predict the stress strain and the stress path correctly.

## CONCLUDING REMARK

The simulation of the triaxial test for Jakarta reddish clay by MC, hardening soil, and soft soil models give the

results that none of the model can predict the stress strain, the pore pressure, and the stress path correctly. Hypothesis on the causes of the discrepancies on the soil models response compared to the actual data is:

- Improper sample preparation.
- Soils of the volcanic origin really have different behavior compared to sedimentary soil.

Considering the simulation was only done on three similar samples, it is too early to draw firm conclusions, further tests, simulation and analysis need to be done.

#### ACKNOWLEDGEMENTS

Finally, the author wishes to thank the organizing committee of this conference, especially Prof. Paulus P. Rahardjo, for inviting the author to write this paper.

#### REFERENCES

- Atkinson, J., 1993, An Introduction to The Mechanics of Soils and Foundation, Mc Graw Hill Book Co, London
- Brinkgrieve, R.B.J., Broere W, Waterman, D, 2011, Plaxis 2D version 2011 manual, Delf, the Netherlands.
- Desai, C.S. and Siriwardane, H.J., 1984, Constitutive Laws for Engineering Materials with Emphasis on Geologic Materials, Prentice Hall, New Jersey.
- Duncan, J.M, and Chang, C.Y., 1970, Non Linear Analysis of Stress and Strain in Soils, Jour. Soil Mech. And Foundations Division, Proc. ASCE.
- Duncan, J.M., Byrne, P., and Wong, K.S., 1980, Strength, Stress-Strain and Bulk Modulus Parameters for Finite Element Analyses of Stresses and Movements in Soil Masses, Report No. UCB/GT/80-01, College of Engineering, Office of Research Services, University of California, Berkeley, California.